Defence Science Journal, Vol. 75, No. 5, September 2025, pp. 588-596, DOI : 10.14429/dsj.20783

A High Transmission Coefficient, Ultra-Low Noise and Wideband LNA for Use in Defence Applications

Subham Banerjee[!,*], Arun Kumar Ray[$] and Santanu Mondal[#]

[!]*RVS College of Engineering and Technology, Jamshedpur - 831 001, India*
[$]*DRDO-Integrated Test Range, Chandipur - 756 025, India*
[#]*Institute of Radio Physics & Electronics, University of Calcutta, Kolkata - 700 009, India*
[*]*E-mail: subham.banerjee@rvscollege.ac.in*

ABSTRACT

The echo signal amplitude received by radar is very low, necessitating signal amplification for effective detection and processing. A Low Noise Amplifier (LNA) has been developed to boost signal amplitude without adding extra noise. This paper presents innovative techniques such as gm-boosting, RC coupling, an L-type matching network, and common source inductive degeneration. These techniques achieve a wide bandwidth of 1.3 GHz (4.7 to 6 GHz) and a low undesired signal level of 0.8 dB. The bias network enhances transconductance, resulting in a gain of 36-40 dB, while the RC coupling network ensures stability from DC to 36 GHz. The LNA achieves an output 1 dB compression point of 9 dBm, an OIP3 of 23.91 dBm, a sensitivity of -137.8 dBm, a linear dynamic range of 108.8 dB, and a spurious free dynamic range of 87.87 dB. This LNA operates well in RF interference environments and demonstrates strong detection capability and linearity. Built on GaAs technology, the MMIC circuit has a compact footprint of 3.5052 mm². This efficient LNA boosts the tracking range from 128 km to 243 km when integrated into larger systems.

Keywords: Dynamic range; Linearity; Stability; Transmission coefficient; Undesired signal level

NOMENCLATURE

f	: Frequency
ω	: Angular frequency
V_{dd}	: Power supply voltage
k_B	: Boltzmann constant
T	: Temperature (in Kelvin)
imn	: Input matching network
C_B	: DC blockin g capacitor
C_C	: Coupling capacitor
L_g	: Gate-biasing inductor
L_d	: Drain-biasing inductor
L	: Inductor at source terminal of the transistor
C	: Capacitor at source terminal of the transistor
M_1	: First stage transistor
M_2	: Second stage transistor
M_3	: Third stage transistor
Z_{in}	: Input impedance
Z_{out}	: Output impedance
Z_0	: Characteristic impedance (=50 Ω)
omn	: Output matching network
A	: Gain of LNA
e	: Noise voltage
i	: Noise current
NF	: Noise Figure

Received : 24 February 2025, Revised : 02 July 2025
Accepted : 07 August 2025, Online published : 01 September 2025

1. INTRODUCTION

Radar communication is essential for military purposes. It is primarily utilized for detecting enemy targets and tracking airborne vehicles during testing scenarios. Low Noise Amplifiers (LNAs) are employed to amplify signals while adding minimal noise, which enhances signal sensitivity. LNAs are positioned at the front end of radar receivers, making them critically important devices in the defense industry.

A Low Noise Amplifier (LNA) was designed to operate at 5 GHz with low power dissipation, but it exhibited a high undesired signal level of 1.4 dB[1]. A wideband LNA utilizing feedback topology[2] was developed to achieve a transmission coefficient of 22.5-25.5 dB and an undesired signal level of less than 1.8 dB. Another LNA designed for 5 GHz demonstrated a significantly lower undesired signal level of 0.6 dB, along with a transmission coefficient of 13 dB[3]. Additionally, a 6 GHz LNA achieved an undesired signal level of 2.66 dB and a transmission coefficient of 12.29 dB at a DC supply of 3 V[4]. The LNA[5] designed to accomplish a transmission coefficient ranging from 15 to 18 dB, with an in-band undesired signal level between 0.9 and 1.6 dB.

The low-noise amplifier (LNA)[6] designed to produce an undesired signal level of 2.4 dB, with a transmission coefficient of 12.3 dB, S11 of -6 dB, and S22 of -16 dB at a frequency of 6 GHz. A 5 GHz LNA[7] yielded an undesired signal level of 2.3 dB and a transmission coefficient of 23 dB. The LNA[8] achieved an undesired signal level of 0.76 dB and

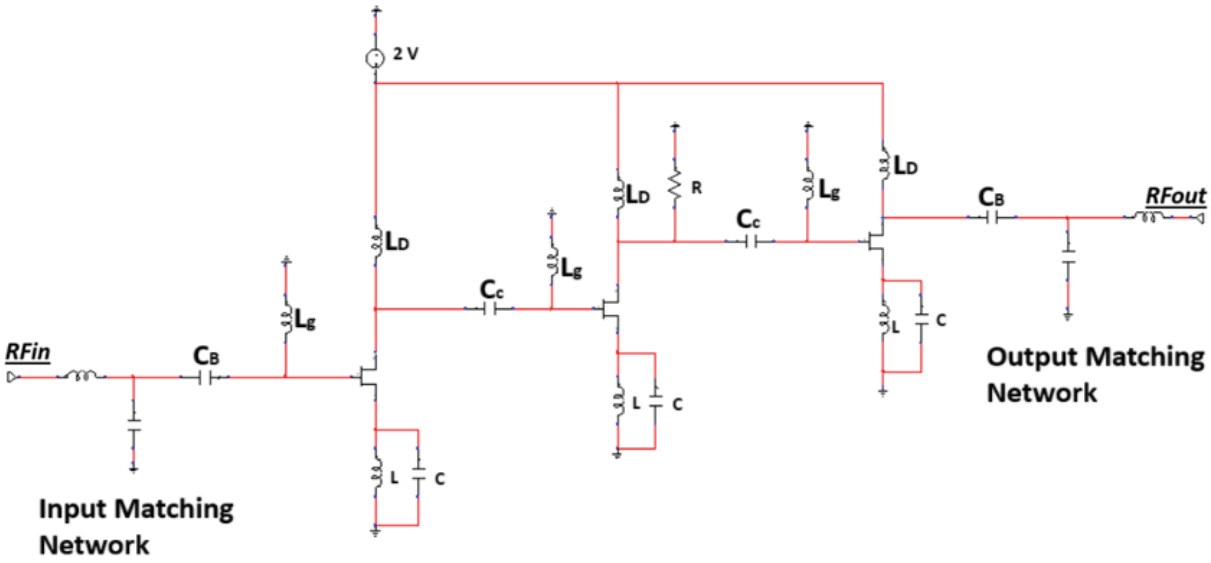

Figure 1. Topology of proposed three stage cascaded C-Band LNA.

a transmission coefficient of over 16 dB at a 3 V operation. A C-band LNA[9] designed to provide a transmission coefficient of 19.1 dB and an undesired signal level ranging from 1.8 dB to 2.6 dB. Additionally, a C-band GaAs-based MESFET was employed to design an LNA that exhibited an undesired signal level of 1.9 dB from a 3 V DC supply[10]. Lastly, a common gate LNA utilizing GaN HEMT demonstrated a transmission coefficient of 25.5 dB and an undesired signal level of 2.1 dB at 5 GHz[11].

A C-Band GaN front-end[12] is designed with a transmission coefficient of 35 dB and a undesired signal level of 3.2 dB at 5.25-5.57 GHz and occupies an area of 7 x 7 mm^2. The LNA[13] gave 18 dB transmission coefficient with 2 dB undesired signal level at 5.9 GHz. Two 5-7 GHz LNAs[14] with a undesired signal level of 1.3 dB and 1.5 dB and transmission coefficient of 15 dB and 16 dB were designed. A self-biased circuit[15] achieved a undesired signal level of 1.37-1.72 dB with transmission coefficient of 18.9 dB and IIP3 of -7.1 dBm. Another self-biased circuit[16] achieved a undesired signal level of 1.35-1.7 dB and a transmission coefficient of 10.9 dB and IIP3 of -5.6 dBm. The proposed design is superior in terms of undesired signal level and transmission coefficient. The proposed design demonstrates superior performance in terms of undesired signal level and transmission coefficient.

Superior results were obtained only with a 2 V power supply. This design features a three-stage low noise amplifier (LNA) that employs a combination of gm-boosting RC coupling, input/output matching techniques, and common source inductive degeneration. These methods result in an ultra-low undesired signal level of 0.8 dB and a very high transmission coefficient of 36-40 dB, while maintaining unconditional stability. Both S11 and S22 are below -10 dB across the entire frequency band.

The output P1dB and the output third-order intercept point (IIP3) are 9 dBm and 23.91 dBm, respectively. The sensitivity of the proposed design is -137.8 dBm, with a linear dynamic range of 108.8 dB and a spurious-free dynamic range of 87.87 dB.

Section 2 provides details on circuit design. Specifically, Section 2.1 demonstrates the various techniques used.

Section 3 presents the footprint and results of electromagnetic simulations, while Section 4 concludes the work.

2. CIRCUIT DESIGN

The miniature circuit is designed using GaAs pHEMT technology with a gate length of 0.15 µm. This paper presents a C-Band low noise amplifier (LNA) implemented using 0.15 µm pHEMT technology. The proposed LNA features a three-stage configuration, with each stage connected in a cascaded manner, as illustrated in Fig. 1.

In the first stage, the pHEMT has a number of fingers (NOF) of 8 and a unit gate width (UGW) of 60 µm. The second stage also uses a pHEMT with an NOF of 8 but has a UGW of 25.7 µm. Finally, the third stage's pHEMT has an NOF of 6 and a UGW of 28 µm.

The amplifier employs a self-bias configuration with an LC combination in the transistor's source. An L-type LC matching network is utilized for impedance matching. Furthermore, an interstage RC coupling network with a shunt resistor connects the second and third stages. The value of the resistor in the RC coupling network is set at 139.7 ohms to optimize stability and reduce undesired signal levels.

2.1 Techniques Used

2.1.1 Gm-Boosting Technique for Transmission Coefficient Enhancement

In the Gm-boosting technique, self-biasing is employed to achieve a high transmission coefficient. A suitable biasing network is chosen to obtain an IdQ of 101 mA and a VgsQ of 0 V, which helps achieve a high transmission coefficient and a complete output cycle. An increase in drain current leads to a rise in transconductance, resulting in an even higher transmission coefficient. The maximum drain current and the operating point are illustrated in Fig. 2.

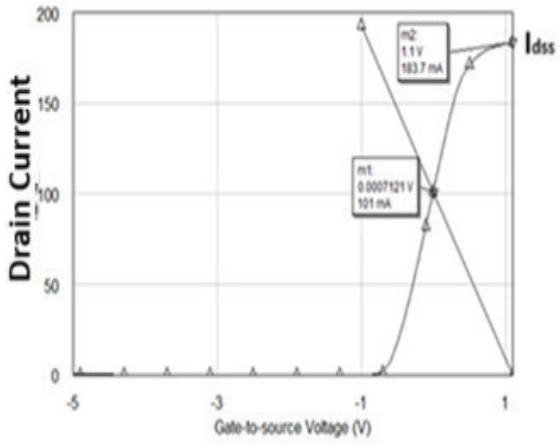

Figure 2. Q-point of the transistor with gate width of 8 x 60 µm.

From Fig. 2, the maximum drain current for the first stage of the LNA is 183.7 mA, with an operating point of IdQ = 101 mA at VgsQ = 0 V. The high transmission coefficient is achieved due to an effective biasing circuit.

The analytical expression for the transmission coefficient is presented below. The ABCD matrices for the input matching network, the first stage, the second stage, the third stage, and the output matching network are provided in Eqn. (1), Eqn. (2), Eqn. (4), Eqn. (6), and Eqn. (7). These ABCD matrices are derived from their corresponding equivalent circuits, as illustrated in Fig. 3, Fig. 4, Fig. 5, and Fig. 6.

The overall ABCD matrix is obtained by multiplying all the individual matrices together. This combined ABCD matrix is then converted into S-parameters. From the S-matrix, the value of S21 can be computed using MATLAB. Figure 3 depicts the input matching network, and the matrix in Eqn. (1) is formulated based on this network.

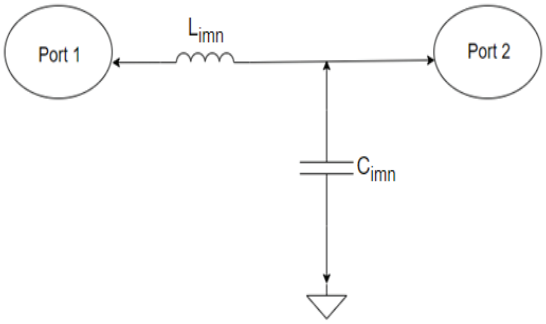

Figure 3. Input matching network.

The ABCD matrix of the input matching network is given in Eqn. (1)

$$A_{imn} = \begin{pmatrix} 1-\omega^2 L_{imn} C_{imn} & j\omega L_{imn} \\ j\omega C_{imn} & 1 \end{pmatrix} \quad (1)$$

The pHEMT in each stage can be replaced by a parallel combination of \(R_{on} \) and \(C_{on} \). According to the equivalent circuit shown in Fig. 4, a novel analytical formula is provided in Eqn. 2. This equivalent circuit consists of the gate inductor \(L_g \) and the drain inductor \(L_d \), which are parallel to each other. The resulting inductance is in parallel with the series connection of the transistor equivalent model (the parallel combination of \(R_{on} \) and \(C_{on} \)) and the inductance-capacitance (LC) circuit at its source terminal.

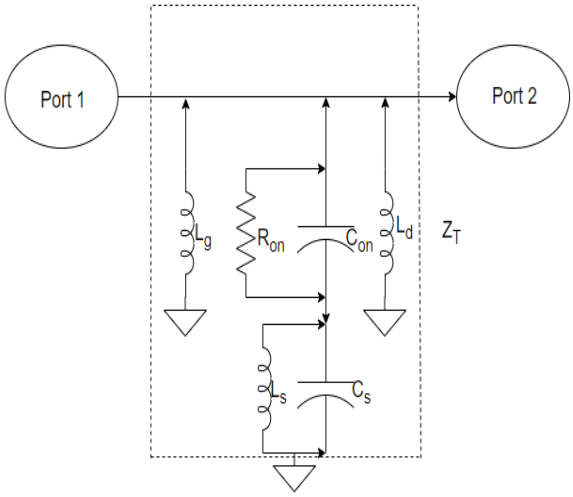

Figure 4. Equivalent circuit of the primary stage of LNA.

The ABCD matrix of the primary stage of LNA is given in Eqn. (2).

$$A_1 = \begin{bmatrix} 1 & 0 \\ \dfrac{1}{Z_T} & 1 \end{bmatrix} \quad (2)$$

$$Z_T = \frac{\dfrac{j\omega L_d L_g}{L_d + L_g}\left(\dfrac{\dfrac{R_{on}}{(\omega C_{on})^2}}{R_{on}^2 + \left(\dfrac{1}{\omega C_{on}}\right)^2} - j\left(\dfrac{\dfrac{R_{on}^2}{\omega C_{on}}}{R_{on}^2 + \left(\dfrac{1}{\omega C_{on}}\right)^2} + \left(\dfrac{\dfrac{L_s}{C_s}}{(\omega L_s) - \left(\dfrac{1}{\omega C_S}\right)}\right)\right)\right)}{\dfrac{\dfrac{R_{on}}{(\omega C_{on})^2}}{R_{on}^2 + \left(\dfrac{1}{\omega C_{on}}\right)^2} + j\left(\dfrac{\omega L_d L_g}{L_d + L_g} - \left(\dfrac{\dfrac{R_{on}^2}{\omega C_{on}}}{R_{on}^2 + \left(\dfrac{1}{\omega C_{on}}\right)^2}\right) - \left(\dfrac{\dfrac{L_s}{C_s}}{(\omega L_s) - \left(\dfrac{1}{\omega C_S}\right)}\right)\right)} \quad (3)$$

The equivalent circuit of Fig. 5 is used to formulate the ABCD matrix of second stage of LNA as shown in Eqn. 4. The same equivalent circuit is used along with the shunt resistor, r.

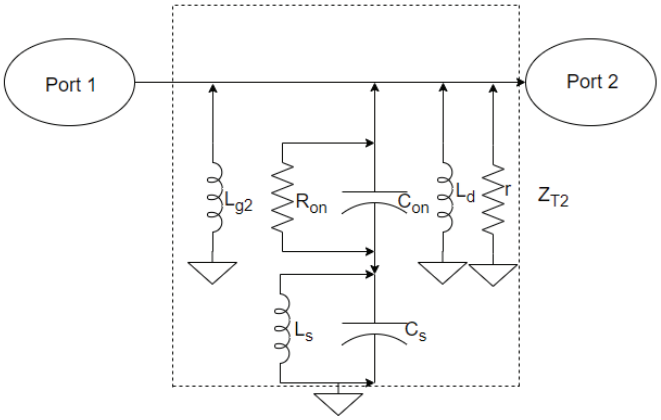

Figure 5. Equivalent circuit of the second stage of LNA.

$$A_1 = \begin{bmatrix} 1 & 0 \\ \dfrac{1}{Z_{T2}} & 1 \end{bmatrix} \quad (4)$$

L_{g2} is the biasing inductor at the gate of pHEMT of the second stage. For second stage of LNA, Z_T is obtained by replacing L_g with L_{g2}.

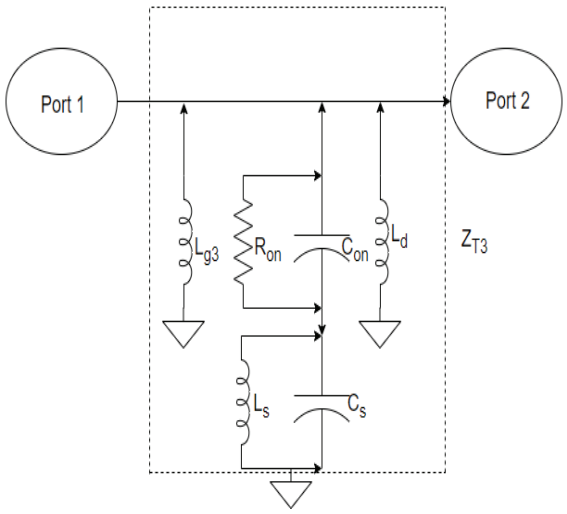

Figure 6. Equivalent circuit of the third stage of LNA.

$$z_{T2} = \frac{rZ_T}{r + Z_T} \tag{5}$$

Figure 6 shows the equivalent diagram of third stage of LNA with L_{g3}, used in place of L_g in Eqn. 3. L_{g3} is the biasing inductor of the third stage.

The ABCD matrix of the third stage of LNA is given in Eqn. (6).

$$A_2 = \begin{bmatrix} 1 & 0 \\ \dfrac{1}{Z_{T3}} & 1 \end{bmatrix} \tag{6}$$

L_{g3} is the biasing inductor at the gate of pHEMT of the third stage. For third stage of LNA, Z_{T3} is obtained by replacing L_g with L_{g3} in Eqn. (3).

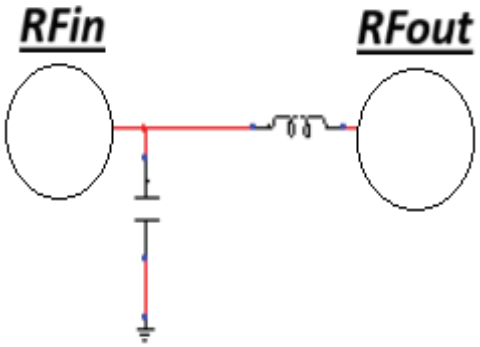

Figure 7. Output matching network of LNA.

The ABCD matrix of the output matching network as shown in Fig. 7 is given in Eqn. (7).

$$A_{omn} = \begin{bmatrix} 1 & j\omega L_{omn} \\ j\omega C_{omn} & 1 - \omega^2 L_{omn} C_{omn} \end{bmatrix} \tag{7}$$

The stages are connected in cascaded fashion. The overall matrix becomes $A_{imn} x A_1 x A_2 x A_3 x A_{omn}$.$S_{21}$ can be calculated from the overall matrix by the formula[17].

$$S_{21} = \frac{2}{A + \dfrac{B}{50} + Cx50) + D} \tag{8}$$

where, A, B, C and D are the parameters of the overall matrix. Analytical results for transmission coefficient matches with the result obtained in the simulation which is shown in Fig. 12 (a). Since, gate voltage is at 0 V, maximum drain current flows through the circuit, leading to high transmission coefficient.

2.1.2 LC Matching Network and Resistor in Parallel to the Second Stage for Undesired Signal Level Reduction

The noise factor of the GaAs pHEMT-based three-stage LNA is given by Frii's formula for noise factor[18]. The undesired signal level is given by NF=10 x log (F) and F is given in Eqn. 9.

$$F = F_1 + \frac{F_2 - 1}{A_1} + \frac{F_3 - 1}{A_1 A_2} \tag{9}$$

A_1 and A_2 are the absolute transmission coefficients of first and second stages, respectively. The noise model for the first stage of LNA with the input matching network is shown in Fig. 8.

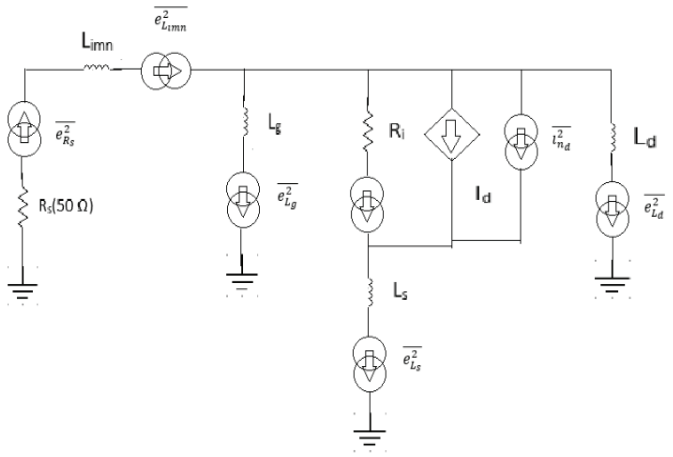

Figure 8. Noise model of single stage C-Band MMIC LNA.

The noise factors F_1, F_2 and F_3 can be expressed in terms of ratio of the noise voltages.

$$F_1 = \frac{E_{t1}^2 + E_{n1}^2 + I_{n1}^2 R_s^2}{E_{t1}^2} \tag{10}$$

$$F_2 = \frac{E_{t2}^2 + E_{n2}^2 + I_{n2}^2 Z_{01}^2}{E_{t2}^2} \tag{11}$$

$$F_3 = \frac{E_{t3}^2 + E_{n3}^2 + I_{n3}^2 Z_{02}^2}{E_{t3}^2} \tag{12}$$

"E" represents noise voltage and "I" represents noise current. Here E_{t1} can be calculated using $E_{t1} = \sqrt{4k_B T R_s \triangle f}$, E_{n1} can be found out using:

$E_{n1} = \sqrt{\left(A_1 \overline{e^2_{ngLimn}}\right)^2 + A_1 \overline{e^2_{ngLg1}}^2 + \overline{e^2_{ndLd}}^2}$, $I_{n1}{}^2$ can be expressed as

$4kT\Delta f g_{m1} P$. g_{m1} is transconductance of the first stage and the value of P is 0.00396. For second stage, E_{t2}, E_{n2} and I_{n2} can be found out from Eqn.s 13, 14 and 15 respectively. Z_{o1} and Z_{o2} are the output impedances of stage 1 and stage 2, respectively.

$$E_{t2} = 4k_B T Z_{out1} \triangle f \tag{13}$$

$$E_{n2} = \sqrt{\left(A_2 \overline{i_{ngLg2}^2}^{\,2} + \overline{i_{ndLd}^2}^{\,2} + \overline{i_{ndr}^2}^{\,2}\right)} \quad (14)$$

$$\overline{i_{n2}^2} = 4k_B T \triangle f g_{m2} P \quad (15)$$

A_2 is the transmission coefficient of the second stage. $\overline{i_{ngLg2}^2}$, $\overline{i_{ndLd}^2}$, $\overline{i_{ndr}^2}$ and is given in Eqn. 16, Eqn. 17 and Eqn. 18.

$$\overline{i_{ngLg2}^2} = 2qI_{d1} \triangle f \quad (16)$$

$$\overline{i_{ndLd}^2} = 2qI_{d2} \triangle f \quad (17)$$

$$\overline{i_{ndr}^2} = 4k_B T \triangle f r \quad (18)$$

I_{d1} and I_{d2} are drain currents of first and second stage respectively. Similarly, for the third stage, E_{t3}, E_{n3} and I_{n3} can be found out from Eqn. 19, Eqn. 20 and Eqn. 21.

$$E_{t3} = 4k_B T \triangle f Z_{out2} \quad (19)$$

$$E_{n3} = \sqrt{\left(A_3 \overline{i_{ngLg3}^2}^{\,2} + \overline{i_{ndLd3}^2}^{\,2}\right)} \quad (20)$$

$$\overline{i_{n3}^2} = 4k_B T \triangle f g_{m3} P \quad (21)$$

A_3 is the transmission coefficient of the third stage. $\overline{i_{ngLg3}^2}$ and $\overline{i_{ndLd3}^2}$ can be found out from Eqn. 22 and Eqn. 23.

$$\overline{i_{ngLg3}^2} = 2qI_{d2} \triangle f \quad (22)$$

$$\overline{i_{ndLd3}^2} = 2qI_{d3} \triangle f \quad (23)$$

The noise factor of the first stage depends on E_{n1} component which in turn depends on L_{imn}. Since input matching inductor is at small value, we achieve very low undesired signal level. L-type LC matching network is also responsible for reduction in undesired signal level.

2.1.3 LC Matching Network for Bandwidth Analysis

L-type input/output LC matching network is used in broadening the bandwidth of LNA. Bandwidth can be determined from the plot of S_{11} with frequency. S_{11} can be determined using input impedance (Z_{in}) from Eqn. 24.

$$Z_{in} = j\omega L_{imn} - \frac{\dfrac{\dfrac{L_g}{\omega C_{gs} C_{imn}} + j\left(\dfrac{\dfrac{L_g}{C_{imn}}}{\omega L_g - \dfrac{1}{\omega C_{imn}}}\right)\left(R_i + \dfrac{\dfrac{L_s}{C_s}}{\omega L_s - \dfrac{1}{\omega C_s}}\right)}{\left(R_i + \dfrac{\dfrac{L_s}{C_s}}{\omega L_s - \dfrac{1}{\omega C_s}}\right) - j\left(\dfrac{1}{\omega C_{gs}} + \dfrac{\dfrac{L_g}{C_{imn}}}{\omega L_g - \dfrac{1}{\omega C_{imn}}}\right)} \quad (24)$$

$$S_{11} = \frac{Z_{in} - 50}{Z_{in} + 50} \quad (25)$$

A bandwidth of 1.3 GHz is obtained in S11 vs frequency plot in Fig. 13. The LC matching network at the input side and the gate inductor of the first stage contribute to a significant improvement of bandwidth. The limitation of LC matching network is narrow bandwidth. In this paper, LC matching network along with biasing network has been implemented to achieve wide bandwidth.

2.1.4 RC Coupling Circuit for Stability of LNA

The proposed design is unconditionally stable from DC to 36 GHz. The resistor, denoted as \(r \), in the second inter-stage RC coupling network plays a crucial role in determining the stability of the Low Noise Amplifier (LNA). Without this resistor, the LNA fails to meet the conditions for unconditional stability. Adding a resistor of significant value increases stability. Furthermore, this resistor also impacts the level of undesired signals in the LNA. Increasing the value of resistor \(r \) leads to a substantial reduction in the level of undesired signals. The resistance value is selected to ensure both a low level of undesired signals and high stability. Figure 9 illustrates the variation of the stability factor with frequency.

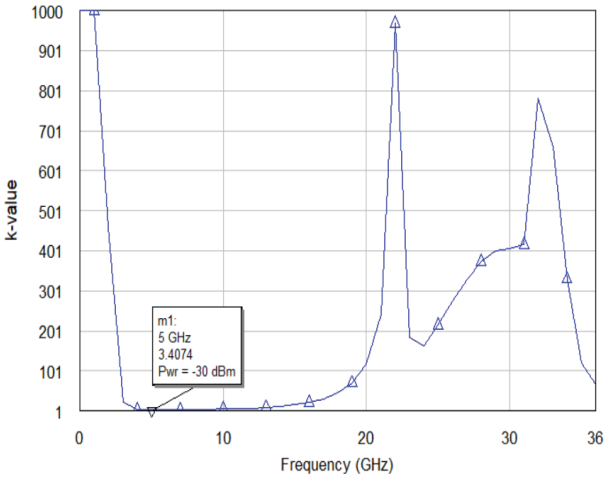

Figure 9. Stability factor with frequency.

An increase in the resistance (r) of the RC coupling network decreases the stability. This also reduces undesired signal level. The value of r (139.7 Ohm) brings high stability and ultra-low undesired signal level.

2.1.5 Inductive Degeneration for Improvement of Input 1 dB Compression and IIP3

The formula expression for drain current of GaAs pHEMT for triode and saturation region are given in Eqn. 26 and Eqn. 27 respectively.

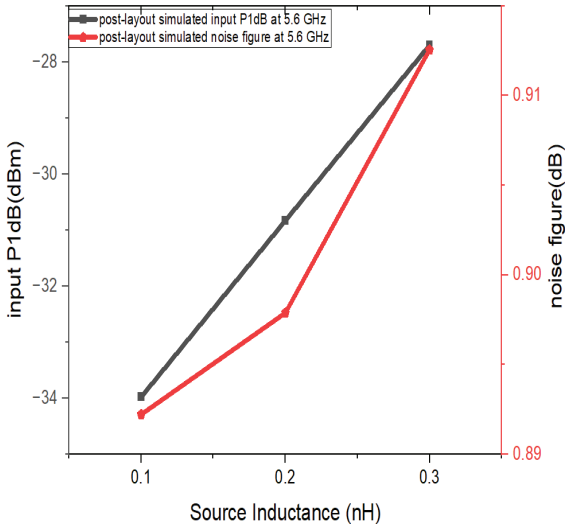

Figure 10. Variation of Input P1dB and undesired signal level of LNA with source inductor.

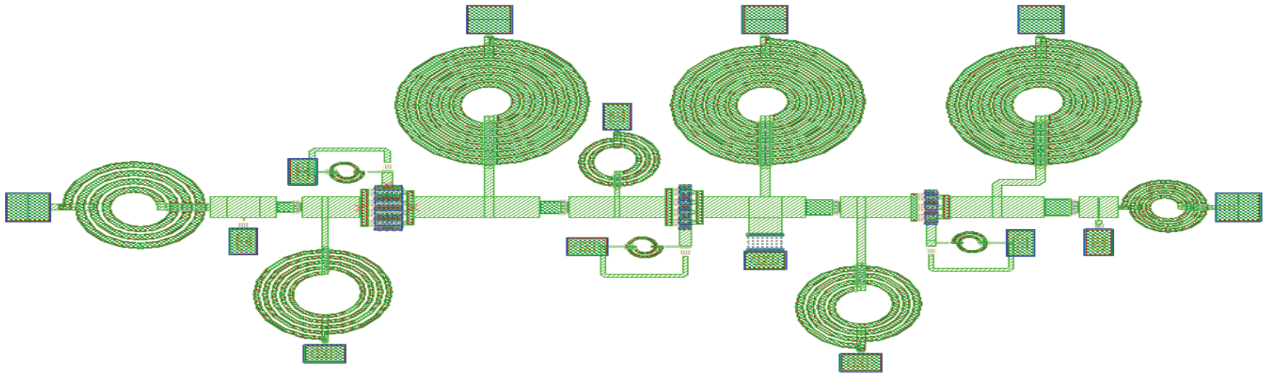

Figure 11. Footprint of the proposed C-Band MMIC LNA (Footprint size-2.76 x 1.27 mm2).

$$I_d = KP\left(\frac{W}{L}\right)\left(V_{gs} - V_{to}\right) V_{ds} - \left[1 + \frac{gamma}{2\sqrt{phi}}\right]\frac{V_{ds}^2}{2} \quad (26)$$

$$I_d = KP\left(\frac{W}{L}\right)\frac{\sqrt{phi}}{2\sqrt{phi} + gamma}\left(V_{gs} - V_{to}\right)^2 \quad (27)$$

Phi (=2) is the surface potential in strong inversion, which is twice the bulk potential. V_{to} (=-1.435 V) is the threshold voltage of the device. V_{gs} depends on the inductor to the source of the transistor. As we increase the value of source inductor, P1dB improves, as seen from Fig. 10.

As per the design, the source inductance is at 0.2 nH. The source inductance of 0.3 nH is not chosen since undesired signal level at that point exceeds 0.9 dB despite improvement in input P1dB. At the source inductance of 0.2 nH, undesired signal level is nearly 0.88 dB and input P1dB at -29 dBm. Thus, inductive degeneration technique improves the linearity of LNA at the cost of gain.

3. FOOTPRINT AND EM SIMULATION RESULTS

The GaAs pHEMT features a gate length of 0.15 µm. In the first stage, it has a gate width of 8 x 60 µm; in the second stage, the gate width is 8 x 25.7 µm; and in the third stage, the gate width is 6 x 28 µm. Post-layout simulations yield a high transmission coefficient between 36 and 40 dB, along with a low undesired signal level of 0.8 dB and unconditional stability. The results of these simulations are illustrated in Fig. 12 to Fig. 15.

Analytical Eqn. for the transmission coefficient are provided in Eqn. 1 to Eqn. 8, while Eqn. 9 to Eqn. 23 relate to the undesired signal level. The plots of these analytical Eqn. can be seen in Fig. 12. It is observed from the graphical representations of both the analytical results and electromagnetic simulations that the outcomes obtained in the post-layout simulations closely match those derived from the analytical expressions.

The transmission coefficient & undesired signal level plots of the proposed design shows good agreement between theoretical and post-layout simulated S-parameters. The S_{11} and S_{22} of the proposed design are better than -10 dB at 4.7-6 GHz frequencies. LNA is properly matched to source and load impedances.

S_{11} & S_{22} vs frequency plot after post lay-.out simulation is shown in Fig-13 which shows a wide bandwidth of 1.3 GHz (from 4.7 to 6 GHz). The LNA shows good linearity

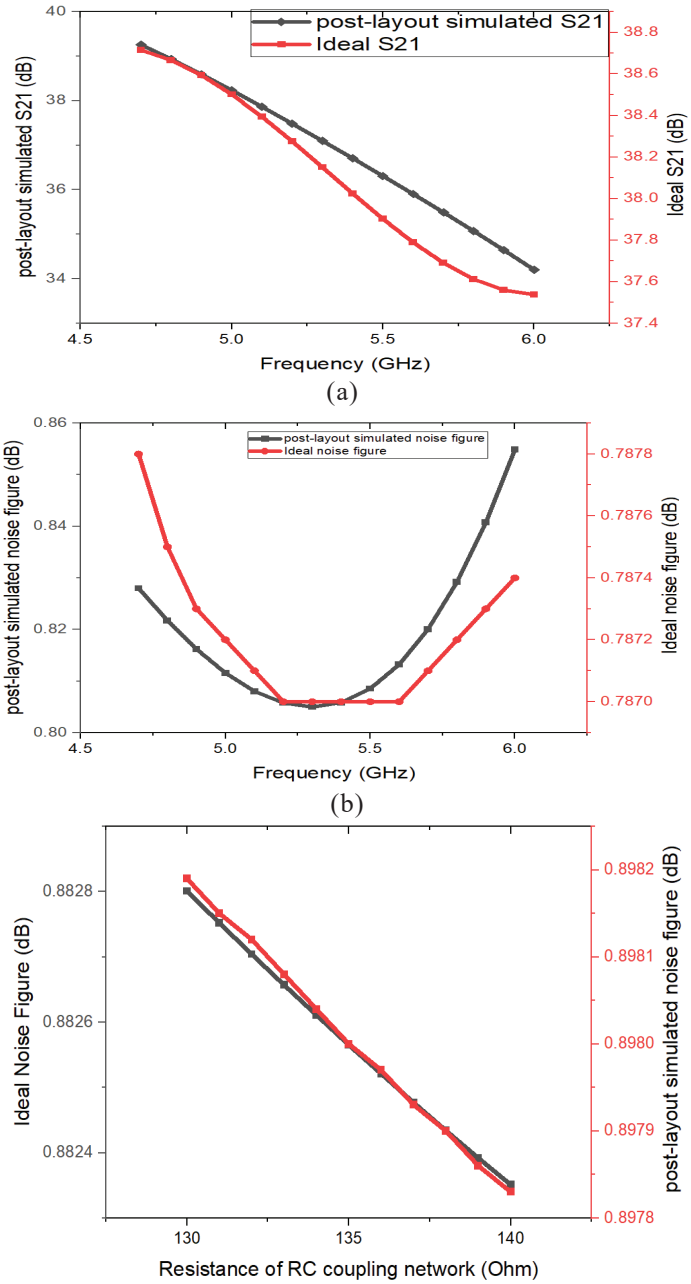

Figure 12. (a) Transmission coefficient with frequency; (b) Undesired signal level with frequency; and (c) Undesired signal level with resistance, r of the RC coupling network.

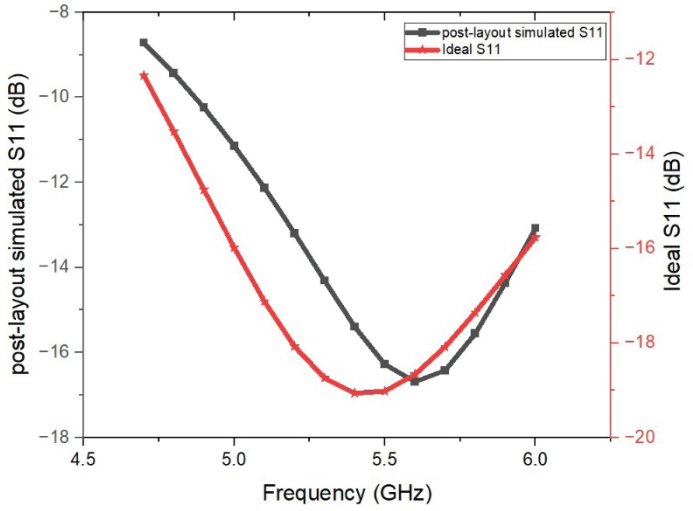

(a)

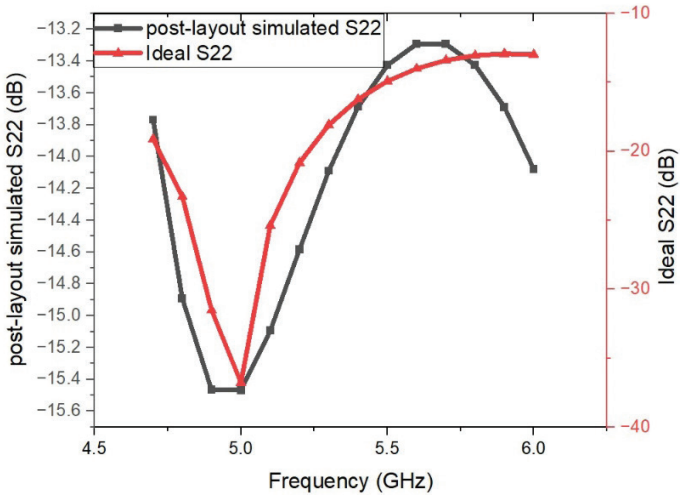

(b)

Figure 13. Plot of reflection coefficients with frequency (a) S_{11}, (b) S_{22}.

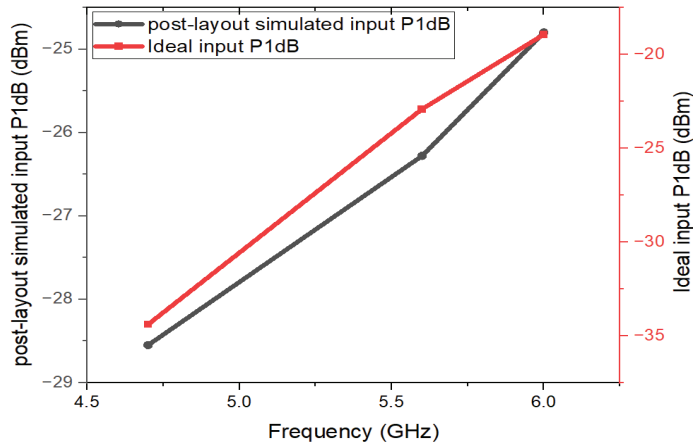

Figure 14. Post-layout simulated and Ideal input P1dB with frequency.

characteristics. We have analysed the nonlinear behavior of the amplifier through output P1dB and OIP3. The plots of 1 dB compression and IP3 were obtained from electromagnetic simulation. The output P1dB and OIP3 are 9 dBm and 23.91 dBm respectively at 5.6 GHz. Sensitivity of LNA is -137.8 dBm and linear dynamic range of 108.8 dB. The LNA shows

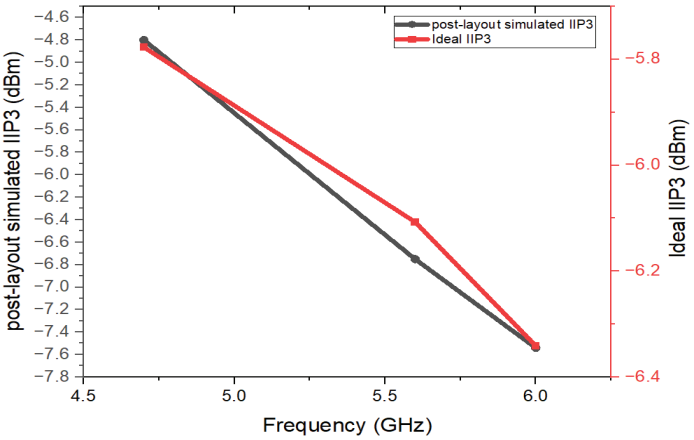

Figure 15. Post-layout simulated and Ideal IIP3 with frequency.

good linearity response in terms of input P1dB (IP1dB) and IIP3 which was obtained from electromagnetic simulation as shown in Fig. 14 and Fig. 15.

The OP1dB of the proposed design is 9 dBm and IIP3 is -6 dBm at 5.6 GHz respectively. The LNA can tolerate upto -29 dBm input power. The gap between 1dB compression point and IIP3 is greater than 10 dB which is commensurate in practical LNA. A comparison in Annexure I is shown which shows the superiority of the proposed design over recent works available in the literature.

4. CONCLUSION

This paper presents the gm-boosting technique that achieves a high gain of 36-40 dB. The L-type LC matching network provides an ultra-low noise figure of 0.8 dB, while the shunt resistor in the RC coupling network ensures unconditional stability. The inductive degeneration technique enhances linearity, specifically input P1dB and IIP3, of the Low-Noise Amplifier (LNA) with a bandwidth of 1.3 GHz in the C-band.

Cascading stages reduces undesired signal levels and improves overall transmission. The figure of merit[27] for this LNA is 38.9757, demonstrating its superior performance. It shows good linear characteristics with a P1dB compression point around -29 dBm and an IIP3 of -6 dBm. The LNA has a sensitivity of -137.8 dBm, a linear dynamic range of 108.8 dB, and a spurious-free dynamic range of 87.87 dB, enhancing the tracking range of C-band radar from 128 km to 243 km.

The LNA operates effectively in RF interference environments and is validated through theoretical and electromagnetic simulations, which align closely despite minor deviations due to microstrip effects and design parameter adjustments.

REFERENCES

1. Wang NY, Khan MZ, Iniewski K. A 0.65V, 1.9MW CMOS low-noise amplifier at 5GHz Internet. 2005. doi: 10.1109/iwsoc.2005.2
2. Abounemra AME, Helaoui M, Ghannouchi FM. A high gain and high linear 0.25 µm GAN HEMT based monolithic integrated C-band low noise amplifier Internet. 2019.

doi: 10.1109/iemantenna.2019.8928801
3. Bergano M, Rocha A, Cupido L, Barbosa D. A 5 GHz LNA for a radio-astronomy experiment Internet. 2011. doi: 10.1109/eurocon.2011.5929355
4. Kamsaini F, Razalli M. Design of C-Band Low-noise Amplifier (LNA) Using E-pHEMT Device for Satellite Communication System. In: 2020 IOP Conf Ser.
5. Molavi R, Mirabbasi S, Hashemi M. A wideband CMOS LNA design approach. 1993 IEEE International Symposium on Circuits and Systems Internet. 2005 Jul 27;48:5107–10. doi: 10.1109/iscas.2005.1465783
6. Zhi-qun C. MMIC LNA based novel composite-channel Al0.3Ga0.7N/Al0.05Ga0.95N/ GaN HEMTS. Chinese Physics. 2007;16(11):3494–7.
7. Aoki Y, Hayama N, Fujii M, Hida H. A 23/3-dB dual-gain low-noise amplifier for 5-GHz-band wireless applications Internet. 2003. doi: 10.1109/gaas.2002.1049059
8. Choi BG, Lee YS, Park CS, Yoon KS. A low noise on-chip matched MMIC LNA of 0.76 dB noise figure at 5 GHz for high speed wireless LAN applications Internet. 2002. doi: 10.1109/gaas.2000.906310
9. Howard DC, Li X, Cressler JD. A low power 1.8–2.6 dB noise figure, SiGe HBT wideband LNA for multiband wireless applications Internet. 2009. doi: 10.1109/bipol.2009.5314152
10. Yoo S, Heo D, Laskar J, Taylor SS. A C-band low power high dynamic range GaAs MESFET low noise amplifier Internet. 2003. doi: 10.1109/rawcon.1999.810962
11. Rao MK, Doemer R, Chevtchenko SA. Common-gate LNA MMIC with Switching Feature Using GaN HEMT for 5G RF front-end. IEEE LMWT. 2023 Oct;33(10):1446–9.
12. Giofre R, Ciccognani W, Colangeli S, Feudale M, Lanzieri C, Polli G. A C-band GaN single chip front-end for SAR applications internet. 2020. doi: 10.1109/rws45077.2020.9050088
13. Triapthi S., Mohapatra B., Tiwari P., Pathak N., & Parida M. Design of RF receiver front end subsystems with low noise amplifier and active mixer for intelligent transportation systems application. Defence Science Journal. 2020;70(6):633–41.
14. Zaid M. et al. Optimizing Low Noise Amplifiers: A Two-Stage Approach for Improved Noise figure and Stability. In: IEEE Access. 2024, 12: 53475-53484. doi: 10.1109/ACCESS.2024.3387108
15. Xiao W, Qiao Y, Liu X, Chen X, Huang C, Guo D. A wideband inductorless LNA utilizing common-source noise-canceling and cascode configuration. Microelectronics Journal Internet. 2024 May 20;150:106252. doi: 10.1016/j.mejo.2024.106252
16. Xiao W, Qiao Y, Liu X, Chen X, Huang C, Guo D. A wideband inductorless LNA exploiting three-stage feedback and thermal noise canceling. Microelectronics Journal Internet. 2024 May 6;149:106237. doi: 10.1016/j.mejo.2024.106237
17. Liang Q, Wang K, Wang X, Yan Y, Liang X. An S–K Band 6-Bit Digital Step Attenuator with Ultra Low Insertion Loss and RMS Amplitude Error in 0.25 μm GaAs p-HEMT Technology. Applied Sciences Internet. 2024 May 1;14(9):3887. doi: 10.3390/app14093887
18. Friis HT. Noise figures of radio receivers. Proceedings of the IRE Internet. 1944 Jul 1;32(7):419–22. doi: 10.1109/jrproc.1944.232049
19. Benboudjema K, Swarup A, Ali K. A C-band low noise amplifier for satellite communications Internet. 1999. doi: 10.1109/mtttwa.1999.755155
20. Harada M. & Tsukahara T. Low dc Power Si-MOSFET L- and C-Band Low Noise Amplifiers Fabricated by SIMOX Technology. IEICE Transactions on Electronics. E82-C, 3: 553-558
21. Yuk JS, Choi BG, Lee YS, Park CS, Kang S. Low-power PHEMT MMIC LNA for C-band applications. Microwave and Optical Technology Letters Internet. 2005 Dec 27;48(2):253–5. doi: 10.1002/mop.21320
22. Salama MK, Soliman AM. 0.7V, 5.745GHz CMOS RF low noise amplifier for IEEE 802.11a wireless LAN. AEU - International Journal of Electronics and Communications Internet. 2009 Jan 21;64(1):29–35. doi: 10.1016/j.aeue.2008.10.003
23. Yadav Y. & Kumar CRS. Design of p-HEMT based Low Noise Amplifier for RF applications in C Band. *IJESIT*, Volume 4, Issue 2, March 2015, 310-320
24. Amer A, Hegazi E, Ragai H. A Low-Power wideband CMOS LNA for WiMAX. IEEE Transactions on Circuits and Systems II Analog and Digital Signal Processing Internet. 2007 Jan 1;54(1):4–8. doi: 10.1109/tcsii.2006.884113
25. Chehrazi S., Mirzaei A., Bagheri R. & Abidi A. A 6.5 GHz wideband CMOS low noise amplifier for multi-band use. *In*Proc. IEEE CICC, Sep. 2005
26. Vishwakarma S., Jank S. & Joo Y. Ultra wide band CMOS low noise amplifier with active input matching. *In*Proc. IEEE Conf. Ultra Wideband Syst. and Technol., May 2004, 415–419
27. Barras D, Ellinger F, Jackel H, Hirt W. A low supply voltage SiGe LNA for ultra-wideband frontends. IEEE Microwave and Wireless Components Letters Internet. 2004 Oct 1;14(10):469–71. doi: 10.1109/lmwc.2004.834556

CONTRIBUTORS

Mr Subham Banerjee is pursuing a PhD at the Institute of Radio Physics & Electronics in Kolkata and working as an Assistant Professor at RVS College of Engineering and Technology in Jamshedpur. His research area focuses on MMIC design.
In this paper, he contributed to reducing the noise figure and performing analytical analysis.

Dr Arun Kumar Ray working as a Scientist-G at DRDO-Integrated Test Range, Chandipur. His research areas include:

MMIC design, tracking radar transmitters, RF front-end systems, and antenna systems.
In this paper, he guided in entire design and drafting process.

Dr Santanu Mondal is an Assistant Professor at the Institute of Radio Physics & Electronics in Kolkata. His research focuses on: Planar monopole antennas, circularly polarized microstrip antennas, reconfigurable antennas, frequency selective surfaces, and microwave absorbers.
In the current study he guided the overall design and drafting process.

Annexure I

Comparison of the proposed work with recent state-of-art

Ref.	Bandwidth (GHz)	Tech.	Transmission coefficient	NF	S_{11}& S_{22}	Stability factor	OP1dB	OIP3	FOM 27	Layout area
12	5 GHz frequency	GaN HEMT	25.5 dB	2.1 dB	-	-	-	-	-	-
13	5.25-5.57 GHz	GaN HEMT	35 dB	3.2 dB	-	-	-	-	-	-
14	5.9 GHz frequency	-	18 dB	2 dB	-20 dB	-	-	-	-	-
19	3.7-4.2 GHz	0.25 µm pHEMT technology	24.5 dB	1.9 dB	< -10 dB	-	6 dBm	18.5 dBm	-	-
20	5.8 GHz	0.25 µm nMOSFET/ SIMOX	7.1 dB	7.4 dB	-	-	-	-	-	-
21	5.8 GHz	0.25 µm pHEMT technology	17 dB	2.55 dB	< - 8 dB	-	-	-	-	-
22	C-Band	0.25 µm CMOS	24.6 dB	5.48 dB	-17.3 dB and -5.3 dB	>> 1	-	-	-	-
23	6 GHz	GaAs pHEMT technology	13.121 dB	0.811 dB	-	-	-	-	-	-
24	0.2-6.2 GHz	0.13 µm CMOS	10.5 dB	2.85 dB	S_{11}< -10 dB	-	-	-	6.48	-
25	0.1-6.5 GHz	0.13 µm CMOS	19 dB	4.2 dB	S_{11} < -10 dB	-	-	-	4.75	-
26	3.1-6.1 GHz	0.18 µm CMOS	17 dB	4.3 dB	S_{11} < -12.9 dB	-	-	-	-	-
This work	4.7-6 GHz	0.15 µm GaAs pHEMT	36-40 dB	0.8 dB	<< -10 dB	>>1 from DC to 36 GHz	9 dBm	23.91 dBm	38.9757	2.76 x 1.27 mm^2